DISPERSION BEHAVIORS OF EXHALED DROPLETS UNDER A DISPLACEMENT VENTILATED ROOM: LAGRANGIAN SIMULATIONS

Gao Naiping[1], He Qibin[1*], Niu Jianlei[2], Zhu Tong[1], Wu Jiazheng[1]
[1]Institute of Refrigeration and Thermal Engineering, School of Mechanical Engineering, Tongji University, Siping Road 1239#，Shanghai, China
[2]Department of Building Services Engineering, The Hong Kong Polytechnic University, Hung Hom, Kowloon, Hong Kong
[*]Corresponding author: heqibin13@hotmail.com, Tel: 86-21-65983867

ABSTRACT:

This paper adopts an Eulerian-Lagrangian approach to investigate the dispersion behaviors of human exhaled droplets under the displacement ventilation in a typical office room. A particle source in-cell (PSI-C) scheme is used to correlate the concentration with the Lagrangian particle trajectories in computational cells. Droplets with size from 0.1-20μm are released from a numerical thermal manikin's (NTM) nose or mouth with different initial momentums and directions. The possible cross-infection risk caused by the exhaled infectious droplets is investigated. It is found that droplets exhaled from the NTM's nose could be caught by its thermal plume whereas droplets exhaled from the NTM's mouth could penetrate the thermal plume. Droplet sizes affect their dispersion behaviors. The cross-infection risk is small and doesn't depend a lot on the ventilation conditions in this study.

INTRODUCTION

In displacement ventilation (DV), cool and clean air at low momentums is introduced into the lower part of the room. Then it is heated by indoor heat sources and rises to the ceiling. The air outlet is generally located at the ceiling. The most specific characteristic of DV is the temperature stratification along the room height. Moreover, if the heat sources are also the gaseous contaminant sources, the pollutants could be transported directly to the upper level of the room and a higher ventilation efficiency than mixing ventilation is achieved (Bjorn & Nielsen, 2002; Brohus & Nielsen, 1996).

However, previous studies demonstrate that at certain conditions human exhaled droplets could be trapped or locked at the breathing zone due to the combined effect of particle initial momentum, particle size, vertical temperature stratification, upward thermal plume around the human body and local air flow conditions. Skistad et al. (2004) believed that if the heat source is also the contaminant source and if the heat source is too weak, the plume might disintegrate at a lower level due the stronger heat plume nearby. So the contaminants will then be trapped at this level and slowly transported indirectly by the stronger convection flows to the upper zone. Bjorn and Nielsen (2002) found that air exhaled through the mouth of a breathing manikin can be "locked" in a thermally stratified layer, where concentrations are several times higher than those at the exhaust. They believed that if the vertical temperature gradient is larger than approximately 0.4-0.5℃/m, this layer can settle into breathing height. Qian et al. (2006) found that a high concentration layer of exhaled droplets nuclei from a bed-lying manikin was observed in DV. Gao et al. (2008) investigated exhaled droplets (0.1-10μm in diameter) under DV system and found that there is a trapped layer of droplets in the breathing zone when droplets are exhaled from the nose. Nevertheless, in these studies, they used either tracer gases to represent droplets or use Eulerian-Eulerian methods to investigate the dispersion behaviors of human exhaled droplets. Moreover, the parametric study of the factors that would influence the mechanism of the lock-up phenomenon is needed to be fully explored.

This paper studies the dispersion behaviours of the exhaled droplets in displacement ventilated rooms and further explores the factors that would influence the mechanism of the lock-up phenomenon using an

Eulerian-Lagrangian approach. A particle source in-cell (PSI-C) scheme is used to correlate the concentration with the Lagrangian particle trajectories in computational cells. The airflow field and particle trajectories are solved with the aid of the Computational Fluid Dynamics (CFD) package Fluent (Fluent 2006) and the particle concentration is dereived through a user-written sub-program. Droplet sizes ranging from 0.1-20μm are exhaled either from a numerical thermal manikin's (NTM) nose or mouth. The spatial distributions of droplets and the cross-infection risk are studied under two exhalation modes and three ventilation conditions.

NUMERICAL METHOD

Airflow model

The general form of the governing equations is as follows:

$$\frac{\partial(\rho\phi)}{\partial t} + div\left(\rho\vec{U}\phi\right) = div\left(\Gamma_\phi grad\phi\right) + S_\phi \qquad (1)$$

Here ϕ represents each of the three air velocity components u, v, and w, the turbulence kinetic energy k, the turbulence dissipation rate ε, and the temperature *T*. When ϕ is unity, Eq. (1) represents conservation of mass. $\vec{U}$ is air velocity vector, ρ air density, Γ_ϕ the effective diffusion coefficient, and S_ϕ the source term of the general form in the governing equations. Given the complexity of combined buoyant flow and forced convective flow indoors, the renormalized group (RNG) k-ε turbulence model with the standard wall function was used to enclose the Navier-Stocks equations.

A surface-to-surface radiation model was used to take the radiative heat transfer into account. Incompressible ideal gas law was adopted to reflect the change of air density to temperature in the momentum equations. The convection and diffusion terms for all variables excpet pressure were discretized by second order upwind and second order central difference scheme. The convection term for pressure was discretized by Pressure Staggering Option (PRESTO) Scheme. The Semi-Implicit Method for Pressure-Linked Equations (SIMPLE) algorithm proposed by Patankar and Spalding (1972) was used to couple the pressure and velocity variables. The turbulence kinetic energy k and turbulence dissipation rate ε employed in air inlets and outlets were calculated by Eq. (2) to (4).

$$k = \frac{3}{2}(u_{avg} I)^2 \qquad (2)$$

$$\varepsilon = C_\mu^{3/4}(k^{3/2} l) \qquad (3)$$

$$l = 0.07 D_h \qquad (4)$$

where u_{avg} refers to the mean flow velocity, I is the turbulence intensity, D_h is the hydraulic diameter, and $C_\mu = 0.09$.

Lagrangian particle tracking model

The Lagrangian particle tracking method calculates individual trajectory by solving the particle momentum equation. By equating the particle inertia with external forces, the momentum equation can be expressed as:

$$\frac{du_P}{dt} = \frac{1}{\tau}\frac{C_D \,\mathrm{Re}_P}{24}(u - u_P) + \frac{g(\rho_P - \rho)}{\rho_P} + F_a \qquad (5)$$

In Eq. (5), the left-hand side represents the inertial force per unit mass (m/s^2). The first term on the right-hand side is the drag force. τ is particle relaxation time and C_D is drag coefficient. Re_P is the particle Reynolds number. The second term represents the gravity and buoyancy, where ρ and ρ_P are the density of air and the particle, respectively. F_a stands for additional forces (per unit mass) that may be important. For the current study, the additional forces F_a can be expressed by the sum of Brownian force, thermophoretic force, and the Saffman's lift force.

In the Lagrangian method, the time-averaged flow field determines the mean path of particles, while the fluctuating flow field governs each particle's turbulent dispersion from the mean trajectory. Since the RNG k-ε model can only predict the time-averaged flow field, a discrete random walk

(DRW) model was used to generate the stochastic velocity fluctuations of the airflow field. The DRW model assumes that the fluctuating velocities follow a Gaussian probability distribution. For isotropic RNG k-ε model, the fluctuating velocity components u' have the following form:

$$u' = \zeta\sqrt{\overline{u'^2}} = \sqrt{2k/3} \quad (6)$$

where ζ is the normally distributed random number, and $\sqrt{\overline{u'^2}}$ the local root-mean-square (RMS) value of the velocity fluctuations.

Particle concentration calculation

Since the Lagrangian method couldn't give the particle concentration information directly, a particle source in-cell (PSI-C) sub-routine developed by Zhang and Chen (2006) was used to correlate the concentration with the Lagrangian particle trajectories in computational cells. The formula of the PSI-C scheme is:

$$\overline{C_j} = \frac{\dot{M}\sum_{i=1}^{n} dt_{(i,j)}}{V_j} \quad (7)$$

where $\overline{C_j}$ is particle concentration in the j th cell (particle/m^3 or kg/m^3), $\dot{M}$ is the number or mass flow rate of each trajectory (particle/(s×trajectory) or kg/ (s×trajectory)), V_j is the volume of the j th cell (m^3), $dt_{(i,j)}$ is the particle residence time of the i th trajectory in the j th cell (s).

CASE DESCRIPTION AND BOUNDARY CONDITIONS

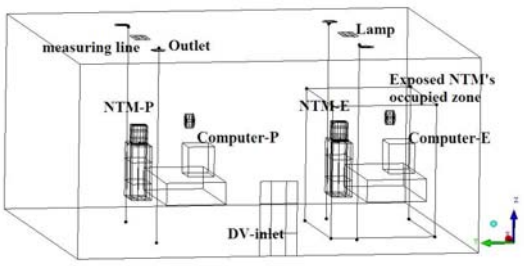

Figure 1 Configuration of the simulated office

Table 1: Detailed boundary conditions

CASE	EXHALED AIRFLOW NTM-P	EXHALED AIRFLOW NTM-E	DV INLET	HEAT SOURCES
Case-1	FR: 6 l/min (nose) V_y: -0.5m/s V_z: -0.5m/s	FR: 6l/min (nose) V_y: -0.5m/s V_z: -0.5m/s	FR: 80 l/s V: 0.16m/s T: 20°C	C-E: 198W; C-P: 198W; NTM-E:75W; NTM-P:75W Lamp:18W×2
Case-2	FR: 12 l/min (mouth) V_y: -1m/s	FR: 6 l/min (nose) V_y: -0.5m/s V_z: -0.5m/s	FR: 80 l/s V: 0.16m/s T: 20°C	C-E:198W; C-P: 198W; NTM-E:75W; NTM-P:75W Lamp:18W×2
Case-3	FR: 6 l/min (nose) V_y: -0.5m/s V_z: -0.5m/s	FR: 6 l/min (nose) V_y: -0.5m/s V_z: -0.5m/s	FR: 80 l/s V: 0.16m/s T: 22°C	C-E: 198W; NTM-E:75W; NTM-P:75W Lamp:18W×2
Case-4	FR: 12 l/min (mouth) V_y: -1m/s	FR: 6 l/min (nose) V_y: -0.5m/s V_z: -0.5m/s	FR: 80 l/s V: 0.16m/s T: 22°C	C-E: 198W; NTM-E:75W; NTM-P:75W Lamp:18W×2
Case-5	FR: 6 l/min (nose) V_y: -0.5m/s V_z: -0.5m/s	FR: 6 l/min (nose) V_y: -0.5m/s V_z: -0.5m/s	FR: 60 l/s V: 0.12m/s T: 18°C	C-E:198W; C-P: 198W; NTM-E:75W; NTM-P:75W Lamp:18W×2
Case-6	FR: 12 l/min (mouth) V_y: -1m/s	FR: 6 l/min (nose) V_y: -0.5m/s V_z: -0.5m/s	FR: 60 l/s V: 0.12m/s T: 18°C	C-E:198W; C-P: 198W; NTM-E:75W; NTM-P:75W Lamp:18W×2

Note: FR: flow rate; C-E: computer for the exposed NTM; C-P: computer for the polluting NTM; NTM-E: the exposed NTM; NTM-P: the polluting NTM.

The dimensions of the simulated office room are width (X) 4.8m×length (Y) 5.4m×height (Z) 2.6m. The origin of the coordinate system was selected at the center of the floor plane (Fig.1). Two numerical thermal manikins (NTM) (75W each) were identical in shape and were seated upright at the tables. Two exhalation jets with different initial momentums and directions were considered here to study the influence of different normal exhalation modes on the dispersion of exhaled droplets. The back NTM

was a polluting source (denoted as P) which exhaled infected airflow either at 6 l/min and 35℃ through the nose (20×10 mm) at 45° degree downward or at 12 l/min and 35℃ through the mouth (20×10 mm) horizontally. The front NTM was an exposed person (denoted as E) which exhaled airflow at 6 l/min through the nose (20×10 mm) at 45° degree downward. Two computers (198W each) and two lamps (18W each) were set as other heat sources. A rectangular opening (500×1000mm) as DV inlet was located at one side wall. The room air was exhausted from four outlets on the ceiling. A cuboid occupied zone of the exposed NTM was chosen to investigate the pollutant concentration in the vicinity of him.

The wall, ceiling and floor of the simulated office were assumed adiabatic and all cooling loads were from internal heat sources. Different thermal conditions and air change rates that would result in various temperature stratification characteristics and local airflow patterns were studied (see Table 1). Average temperatures at the outlets were kept at around 26℃ for all the six cases.

According to the recent findings on respiratory aerosls (Morawska et al. 2009; Chao et al. 2009), we chose to simulate 0.1μm, 1μm, 5μm, 10μm and 20μm droplets as well as tracer gas (CO_2) exhaled from the polluting NTM to study the influence of droplet diameters on the dispersion characteristics. The density of droplets was set as 1000 kg/m^3 and the evaporation process was not considered. The droplet generating rate of the polluting NTM was 100 particles per second.

Due to the stochastic characteristic of the Lagrangian DRW model, it is necessary to test the stabilities of different trajectory numbers. In this study, 8000 trajectories were found to be sufficient to reach the statistically steady state. The fluid-particle interaction was assumed as one-way coupling. The initial velocities and temperatures of the droplets were equal to the exhaled airflows. During particle tracking, if one particle reached inlet, walls, and outlets, its trajectory calculation was terminated.

Hybrid mesh scheme was used to generate grid systems. The unstructured tetrahedral meshes were created in the occupied zone of the NTMs whereas the hexahedral mesh style was used for the rest of the room. 416,752 cells were used to discretize the computational domain. Grid independence test and model validation of both the flow field and droplets concentration field can be found in He et al. (2011) and Gao et al. (2009).

RESULTS AND DISCUSSION

Influence of exhalation airflow on droplets dispersion characteristics

It is observed from Fig.2-a that there are traditional two-zone distributions of contaminants for tracer gas and droplets up to 5μm. In Fig.2, for tracer gas, the concentration in the exhaled air is denoted as 1.0. The droplets exhaled from the NTM's nose could be caught by its thermal plume. Bjorn and Nielsen (2002) used the stratification height (the height where the cumulative volumetric flow rate of the convective flows equal the volumetric flow rate from the inlet) to distinguish the lower clean zone and the upper polluting zone. The stratification height is about 2.0m in case-1 and case-2. The NTM's upward thermal plume could carry tracer gas and small droplets (<5μm) to the upper layer of the room. The concentration distributions for 10μm and 20μm droplets are different from tracer gas and small droplets. Due to their relatively large gravitational forces, the NTM's upward thermal plume couldn't fully bring large droplets to the upper layer. The concentration levels for 10μm and 20μm droplets in the breathing height (1.2-1.8m) are much higher than tracer gas and small droplets.

From Fig.2-b we can observe that the concentration distributions of droplets exhaled from the NTM's mouth with relatively high initial momentums are different from case-1. For tracer gas and small droplets, there are maximum concentrations in the height between 1.6-2.0m. For 10μm droplets, maximum concentrations exist in the height between 1.6-1.8m. For 20μm droplets, two peak concentrations appear, one is in the height between 1.2-1.4m and the other between 1.6-1.8m. Generally, averge concentrations at the four measuring lines in

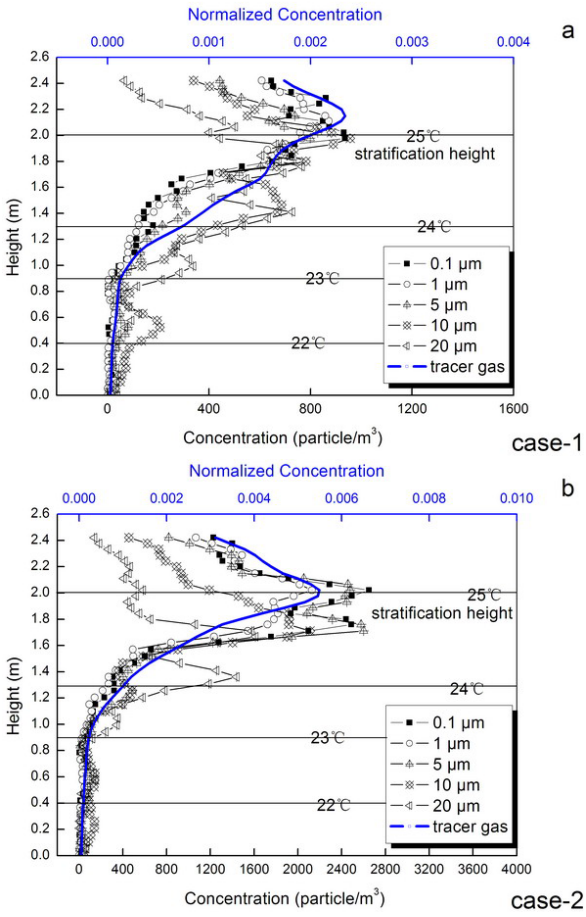

Fig.2 Average droplet concentrations of the four measuring lines (a) case-1; (b) case-2.

case-2 are higher than in case-1. This is because with high initial momentum of the exhalation jet, the exhaled droplets could penetrate the NTM's thermal plume and disperse a longer distance in case-2. The movement of the exhaled droplets affected by the buoyancy exhalation jet, main room air flow, thermal plumes of the polluting NTM and computer as well as the gravitational force and other forces acted on them.

Inspections on the typical trajectoris of 0.1μm particles in case-1 and case-2 (the figures are not shown here due to the space limitation) indicate that droplets exhaled from the NTM's nose could be caught by its thermal plume. Then the droplets disperse horizontally at the upper zone of the room. The movements of the droplets exhaled from the NTM's mouth are more complicated in case-2. It is found that the droplets trajectories are mainly between the polluting NTM and the computer in the front, implying that besides the buoyant exhalation jet, the thermal plumes of the polluting NTM and the computer would affect the transport of mouth-exhaled droplets. This will be further investigated in the next sections. Another finding in case-1 and case-2 is that there are little trajectories that would arrive at the occupied zone of the exposed NTM. It suggests that there is little risk of cross-infection between the two manikins in the current DV system.

Influence of heat sources on droplets dispersion characteristics

In case-3 and case-4, we turned the computer for the polluting NTM off to investigate the influence of local heat sources on droplets dispersion. The temperatures of the supply air for case-3 and case-4 are higher than that of case-1 and case-2 which result smaller vertical temperature gradient in the room. In Fig.3, we used 0.1μm droplets to represent small droplets (<5μm). In case-3, concentrations of small droplets also present a typical two-zone distribution. The stratification height in case-3 is 1.8m which is about 0.2m lower than in case-1. It is found that the concentration levels for small droplets in the breathing height (1.2-1.8m) in case-3 are a little lower than in case-1. This is because due to the smoother vertical gradient, the NTM's thermal plume is stronger in case-3 than in case-1 (Danielsson, 1987). The stronger thermal plume could carry more small droplets into the upper polluting zone. For large droplets, there are also maximum concentrations in the breathing height. The maximum concentration for 20μm droplets appears lower than for 10μm droplets because of larger gravitational force. In case-3, although a stronger NTM's thermal plume exists, it still couldn't fully carry the large droplets to the upper zone.

From Fig.3-b, it is observed that the distributions of droplets exhaled from the mouth in case-4 are different from that in case-2. The concentrations for small droplets are increased with room height. The main differences between case-2 and case-4 are local airflow patterns near the polluting NTM. The airflow pattern in front of the polluting NTM is mainly

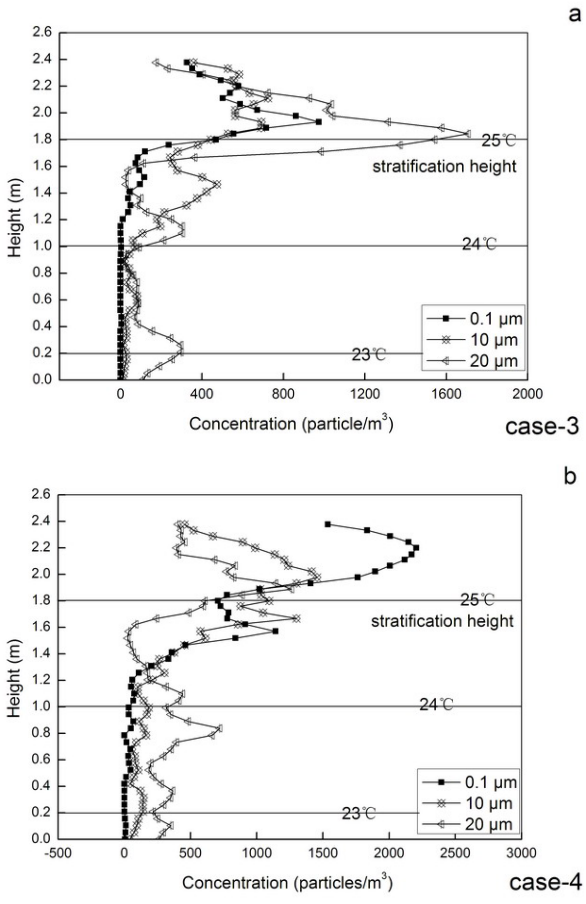

Fig.3 Average droplet concentrations of the four measuring lines (a) case-3; (b) case-4

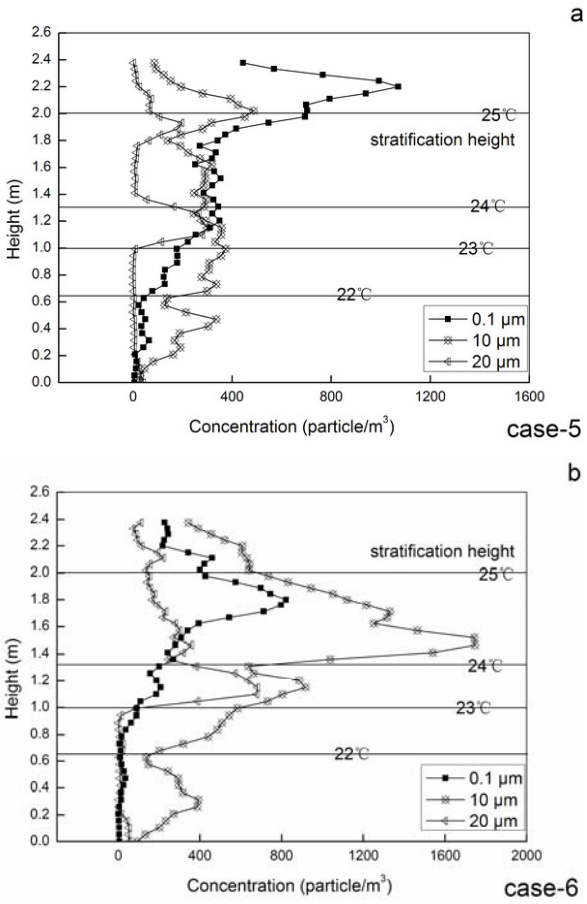

Fig.4 Average droplet concentrations of the four measuring lines (a) case-5; (b) case-6

upward in case-4 and there are some downward counter flows in case-2 owing to the interaction of two thermal plumes. The concentration distribution for 10μm droplets is similar as small droplets. However, 20μm droplets are more likely to move downward.

Influence of air change rate on droplets dispersion characteristics

In this section, we reduced the airflow rate and temperature of the supply air to evaluate their impact on the dispersion of exhaled droplets. Owing to larger temperature differences between the supply and exhaust air, the vertical temperature gradients in case-5 and case-6 are steeper than in case-1 and case-2. From Fig.4-a it is found that there is still two-zone distribution for small droplets exhaled from the NTM's nose, whereas the concentration level is much higher in the lower zone than that in case-1 (i.e. the 0.1μm concentration at 1.4m in case-1 is 143 particle/m^3 whereas it is 285 particle/m^3 in case-5). For 10μm droplets, the concentration is almost uniformly distributed along the room height. For 20μm droplets, a peak concentration appears in the height between 1.0-1.4m. This is because the NTM's thermal plume in case-5 is weaker than in case-1.Therefore, the force for transporting droplets to the upper zone is not significant. These also illustrate the dispersion of droplets exhaled from the NTM's nose depending on its thermal plume a lot. From Fig.4-b it is observed that all droplets are locked up at certain heights in case-6. The larger the droplet size, the lower the maximum concentration. The lock-up heights in case-6 are lower than in case-1 for all droplets sizes.

Cross-infection of exhaled droplets

Due to the discrete characteristic of the Lagrangian DRW model, it is hard to determine the inhaled

concentration for the exposed NTM directly. Instead, we used an alternative index i.e. imagery intake fraction (*IIF*) of the exposed NTM to evaluate the cross-infection risk of the exhaled droplets. Intake fraction is defined as (Nazaroff, 2004):

$$IF = \frac{C_E M_E}{C_P M_P} \quad (8)$$

in which C_P, C_E are the average pollutant concentrations at the mouth of the exposed and the polluting NTM, individually. M_E is the volume flow rate inhaled by the exposed NTM (assuming 6 l/min here), and M_P is the volume flow rate exhaled by the polluting NTM. In this paper, because it is difficult to get C_E, we use the average concentration in the exposed NTM's occupied zone $\bar{C}_{EO}$ to represent C_E and get the imagery intake fraction (*IIF*) as:

$$IIF = \frac{\bar{C}_{EO} M_E}{C_P M_P} \quad (9)$$

From Fig.5, it is found that the imagery intake fractions are almost the same for all the six cases when droplets sizes are smaller than 10μm except in case-3. In case-3, the strong thermal plume of the polluting NTM could bring most droplets to the upper zone and let them removed by the exhausted airflows. The *IIF*s for 10μm droplets are higher than small droplets. For 20μm droplets, there is no droplet that could reach the exposed NTM's occupied zone. From the results of the *IIF* for the six cases studied in this paper, we could deduce that under normal breathing conditions, the exhalation mode and ventilation conditions affect the cross-infection between occupants very little. Gao et al. (2008) suspected that the lock-up of droplets in the breathing zone under DV would increase human exposure risk. In this study, we found that this phenomenon in the breathing zone would increase human exposures only when they are very close to the polluting NTM.

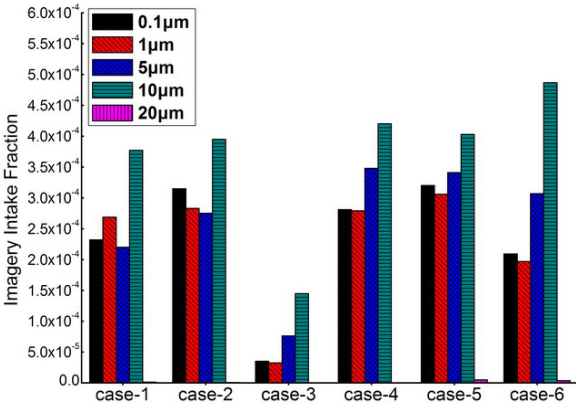

Fig. 5 Imagery intake fraction of the exposed NTM

It should be noted that, because of the protection role of the occupant's thermal plume (Brohus & Nielsen, 1996), the actual intake fraction for the exposed NTM (He, et al., 2011) should be smaller than the imagery intake fraction proposed here.

CONCLUSIONS

This paper adopts an Eulerian-Lagrangian approach to investigate the dispersion behaviors of the exhaled droplets under DV system in a typical office room. The main conclusions from this study are as follows.

1. Droplets exhaled from the NTM's nose could be caught by its thermal plume. The NTM's upward thermal plume could carry tracer gas and small droplets (<5μm) to the upper layer of the room and traditional two-zone distributions of contaminants existed. The stronger the NTM's thermal plume, the more droplets it would carry to the upper layer. The NTM's upward thermal plume couldn't fully bring the 10μm and 20μm droplets to the upper zone due to their large gravitational forces.
2. Droplets exhaled from the NTM's mouth with relatively high momentums could penetrate its thermal plume. The movement of the exhaled droplets is affected by the buoyant exhalation jet, main room air flow, thermal plumes of the polluting NTM and computer as well as the gravitational force and other forces acting on the droplets.
3. The cross-infection risks are almost the same for all the six cases except for case-3when droplets sizes are smaller than 10μm. For 20μm droplets, there are no particles that could reach the exposed NTM's occupied zone.

ACKNOWLEDGEMENT

This study was financially supported by the Research Grant Committee, Hong Kong, China, under the project No. RGC GRF 526508 and the National

Natural Science Foundation of China under the project No. 50808133.

REFERENCES

Bjorn, E., & Nielsen, P.V. (2002). Dispersal of exhaled air and personal exposure in displacement ventilated rooms. *Indoor Air,* **12**, 147-164.

Brohus, H., & Nielsen, P.V. (1996). Personal exposure in displacement ventilated rooms. *Indoor Air-Int. J. Indoor Air Qual. Clim.,* **6**, 157-167.

Chao, C.Y.H., Wan, M.P., Morawska, L., Johnson, G.R., Ristovski, Z.D., Hargreaves, M., Mengersen, K., Corbett, S., Li, Y., Xie, X., & Katoshevski, D. (2009). Characterization of expiration air jets and droplet size distributions immediately at the mouth opening. *Journal of Aerosol Science,* **40**, 122-133.

Danielsson, P.O. (1987). Convective flow and temperature in rooms with displacement system. In *ROOMVENT '87*.

Fluent (2006). Fluent 6.3 User's Guide. Lebanon, NH 03766, USA.

Gao, N.P., Niu, J.L., & Morawska, L. (2008). Distribution of respiratory droplets in enclosed environments under different air distribution methods. *Building Simulation,* **1**, 326-335.

Gao, N.P., Niu, J.L., Perino, M., & Heiselberg, P. (2009). The airborne transmission of infection between flats in high-rise residential buildings: Particle simulation. *Building and Environment,* **44**, 402-410.

He, Q.B., Niu, J.L., Gao, N.P., Zhu, T., & Wu, J.Z. (2011). CFD study of exhaled droplet transmission between occupants under different ventilation strategies in a typical office room. *Building and Environment,* **46**, 397-408.

Morawska, L., Johnson, G.R., Ristovski, Z.D., Hargreaves, M., Mengersen, K., Corbett, S., Chao, C.Y.H., Li, Y., & Katoshevski, D. (2009). Size distribution and sites of origin of droplets expelled from the human respiratory tract during expiratory activities. *Journal of Aerosol Science,* **40**, 256-269.

Nazaroff, W.W. (2004). Indoor particle dynamics. *Indoor Air,* **14**, 175-183.

Patankar, S. V. and Spalding, D. B. (1972) A calculation Procedure for Heat, Mass and Momentum Transfer in Three-dimensional Parabolic Flows. Int. J. Heat and Mass Transfer, 15, 1787-1806.

Qian, H., Li, Y., Nielsen, P., Hyldgaard, C., Wong, T., & Chwang, A. (2006). Dispersion of exhaled droplet nuclei in a two-bed hospital ward with three different ventilation systems. *Indoor Air,* **16**, 111-128.

Skistad, H., Mundt, E., Nielsen, P.V., Hagstrom, K., & Railio, J. (2004). *Displacement ventilation in non-industrial premises* (Second edition ed.). Rehva, Brussels.

Zhang, Z., & Chen, Q. (2006). Experimental measurements and numerical simulations of particle transport and distribution in ventilated rooms. *Atmospheric Environment,* **40**, 3396-3408.